Calculation of the Redox Potentials of Iron–Sulfur Proteins: The 2–/3– Couple of $[Fe_4S_4^*Cys_4]$ Clusters in *Peptococcus aerogenes* Ferredoxin, *Azotobacter vinelandii* Ferredoxin I, and *Chromatium vinosum* High-Potential Iron Protein

G. M. Jensen, A. Warshel, and P. J. Stephens*

Department of Chemistry, University of Southern California, Los Angeles, California 90089

Received April 14, 1994; Revised Manuscript Received June 27, 1994®

ABSTRACT: Calculations of the redox potentials of the 2–/3– couples of $[Fe_4S_4^*Cys_4]$ clusters in the iron–sulfur proteins *Peptococcus aerogenes* ferredoxin (*Pa*Fd), *Azotobacter vinelandii* ferredoxin I (*Av*FdI) and *Chromatium vinosum* high potential iron protein (*Cv*HiPIP) based on the Protein Dipoles Langevin Dipoles (PDLD) method are reported. The structures of these proteins have been determined by X-ray crystallography; in the case of *Pa*Fd the structure has recently been revised due to a change in the sequence close to Cluster II. The large differences between the potentials of the $[Fe_4S_4^*Cys_4]$ clusters of *Pa*Fd and *Av*FdI and the potential of the $[Fe_4S_4^*Cys_4]$ cluster of *Cv*HiPIP are successfully modeled and originate principally in differences in the configuration of main-chain amide groups near the clusters. The small difference between the potentials of *Pa*Fd and *Av*FdI is also satisfactorily modeled in the case of Cluster I of *Pa*Fd. Solvent dipoles close to the cluster in *Pa*Fd are an important contributor to its higher potential. The two X-ray structures of *Pa*Fd yield similar results for Cluster I of *Pa*Fd. In contrast, the results for Cluster II differ substantially; for reasons not yet clear, the recently revised structure leads to results in worse agreement with experiment.

Iron–sulfur [Fe-S] proteins (Lovenberg, 1973a,b; Lovenberg, 1977; Spiro, 1982; Cammack, 1992a) occur very widely in nature. Many [Fe-S] proteins have been isolated and characterized. The structures of a substantial number have been studied *via* X-ray crystallography (Howard & Rees, 1991; Cammack, 1992b). $[FeCys_4]$, $[Fe_2S_2^*Cys_4]$, $[Fe_3S_4^*Cys_3]$, $[Fe_4S_4^*Cys_4]$, and $[Fe_4S_4^*Cys_3]$ clusters (S* = inorganic sulfide; Cys = cysteinate) have been crystallographically characterized in one or more proteins. Other [Fe-S] clusters are known to exist in incompletely characterized [Fe-S] proteins, and the full extent of the spectrum of naturally-occurring protein-bound [Fe-S] clusters is not yet defined.

[Fe-S] clusters can express multiple oxidation levels. Redox potentials of [Fe-S] clusters have been measured in many proteins and are dependent on both the nature of the [Fe-S] cluster and its protein environment (Matsubara & Saeki, 1992; Cammack, 1992b). Since the function of the majority of [Fe-S] proteins is either known or assumed to be electron transport, and since redox potentials control both the thermodynamics and kinetics of electron transfer, an understanding of the redox potentials of [Fe-S] clusters is central to the complete analysis of the functional behavior of [Fe-S] proteins. In the work reported here and in following publications, we address the issue of the protein control of the redox potentials of [Fe-S] clusters. Specifically, we attempt to predict the variation in potential of a redox couple of an [Fe-S] cluster arising from the variation of its protein environment. In this paper we focus on the redox potential of the 2–/3– couple of the $[Fe_4S_4^*Cys_4]$ cluster.[1]

The calculational methodology used in this work has been developed by Warshel and co-workers (Warshel & Russell, 1984; Russell & Warshel, 1985; Parson et al., 1990). *Inter alia*, it has been successfully applied to the analysis of the redox potentials of both native and mutant forms of cytochrome *c* (Churg & Warshel, 1986; Cutler et al., 1989; Langen et al., 1992a). In this approach, the protein surrounding the prosthetic group which constitutes the redox site is approximated as an assembly of partially charged, polarizable atoms, while the aqueous solvent is modeled by a grid of orientable permanent dipoles surrounded by a continuum dielectric. The contribution of the protein and solvent environment to the free energy difference of the oxidized and reduced states of the prosthetic group is approximated by the difference in the electrostatic interaction energies of each state with the charges and induced dipoles of protein atoms, with the solvent dipoles, and with the continuum dielectric. With the assumption that the intrinsic (vacuum) redox potential of the prosthetic group is constant, the variation in redox potential with variation in protein is predicted.

Calculations of redox potentials in this manner require protein structures at the atomic level. Since only relative redox potentials are predicted, the structures of two or more proteins containing a given prosthetic group must be available. Initially, therefore, we focus on [Fe-S] proteins for which atomic resolution X-ray structures have been determined and on [Fe-S] clusters which are present in more than one of this group of proteins. Subsequently, we will address the challenge of the larger number of proteins whose sequences and redox potentials are known, but whose three-dimensional structures have not yet been determined.

[4Fe-4S] clusters are heterogeneous: "classical" [4Fe-4S] clusters contain four cysteine (Cys) ligands, but clusters with three Cys ligands are now known (George et al., 1989; Kennedy & Stout, 1992; Adams, 1992). In this paper, we discuss only $[Fe_4S_4^*Cys_4]$ clusters. These clusters can express more than one redox couple (Carter et al., 1972). The 2–/3– and 1–/2–

* Author to whom correspondence should be addressed.

® Abstract published in *Advance ACS Abstracts,* August 15, 1994.

[1] Throughout this paper we define the redox couples of an [Fe-S] cluster in terms of the formal charges of the entire $[Fe_xS_y^*Cys_z]$ complex. Current convention more often refers to the formal charges of the $[Fe_xS_y^*]$ core. Within this convention, the 2–/3– couple of the $[Fe_4S_4^*Cys_4]$ cluster is defined as the 2+/1+ couple.

0006-2960/94/0433-10911$04.50/0

couples are well-known. Since their potentials have (to date) always been below and above 0 mV (vs SHE), respectively,[2] proteins expressing these couples are often referred to as "low-potential" and "high-potential", respectively. In this paper we restrict our attention to the "low-potential", 2–/3– couple.

At this time, several proteins containing $[Fe_4S_4^*Cys_4]$ clusters expressing the 2–/3– couple have been characterized by X-ray crystallography. *Peptococcus aerogenes* ferredoxin (*Pa*Fd) (Adman et al., 1973, 1976) contains two $[Fe_4S_4^*Cys_4]$ clusters whose indistinguishable redox potentials are ~–430 mV (Stombaugh et al., 1976). *Azotobacter vinelandii* ferredoxin I (*Av*FdI) (Stout et al., 1988; Stout, 1988, 1989; Merritt et al., 1993) contains one $[Fe_4S_4^*Cys_4]$ cluster and one $[Fe_3S_4^*Cys_3]$ cluster; the redox potential of the former is ~–650 mV (Iismaa et al., 1991). *Bacillus thermoproteolyticus* ferredoxin (*Bt*Fd) (Fukuyama et al., 1988; Fukuyama et al., 1989) contains a single $[Fe_4S_4^*Cys_4]$ cluster; the redox potential of the extremely similar *Bacillus stearothermophilus* ferredoxin (*Bs*Fd) (Hase et al., 1976) is ~–280 mV (Mullinger et al., 1975). *A. vinelandii* nitrogenase iron protein (*Av*2) (Georgiadis et al., 1992) contains a single $[Fe_4S_4^*Cys_4]$ cluster whose redox potential is ~–280 mV (in the absence of bound nucleotide) (Watt et al., 1986). *Clostridium acidi-urici* ferredoxin (*Ca*Fd) (Krishnamurthy et al., 1988; Tranqui et al., 1991) contains two $[Fe_4S_4^*Cys_4]$ clusters whose indistinguishable redox potentials are ~–440 mV (Rall et al., 1969). Trimethylamine dehydrogenase (TMD) (Lim et al., 1986) contains one $[Fe_4S_4^*Cys_4]$ cluster, together with an FMN prosthetic group; the redox potential of the [Fe-S] cluster is near 0 mV (Pace & Stankovich, 1991). In this paper, we report calculations for the $[Fe_4S_4^*Cys_4]$ clusters of *Pa*Fd and *Av*FdI; *Bt*Fd, *Av*2, *Ca*Fd, and TMD will be discussed in subsequent papers. In order to shed light on the factors causing $[Fe_4S_4^*Cys_4]$ clusters to express either the 2–/3– or 1–/2– couple, we simultaneously report calculations on the 2–/3– couple of a crystallographically characterized "high-potential" protein: specifically, the *Chromatium vinosum* High Potential Iron Protein (*Cv*HiPIP) (Carter et al., 1972, 1974a,b; Freer et al., 1975), which contains a single $[Fe_4S_4^*Cys_4]$ cluster.

Preliminary results and analysis were reported in an earlier Communication (Langen et al., 1992b).

METHODS

Calculations of redox potentials have been carried out using the so-called Protein Dipoles Langevin Dipoles (PDLD) methodology of Warshel and co-workers (Warshel & Russell, 1984; Russell & Warshel, 1985; Parson et al., 1990), implemented in the program POLARIS (Warshel & Creighton, 1989; Lee et al., 1993). Cartesian coordinates for those protein atoms located by X-ray crystallography are obtained in the form of Brookhaven data base files. Non-protein atoms, including water O atoms, are deleted. H atoms are added to all amino acid residues excepting the four Cys cluster ligands using standard geometrical parameters. The $Fe_4S_4^*(S_\gamma)_4$ moiety of the [Fe-S] cluster is defined to be the prosthetic group ("region I"). The protein surrounding region I is truncated using a sphere of radius r_2 centered at the centroid of region I, creating "region II". The protein, as defined by regions I and II, is immersed in a grid of point dipoles, representing water molecules, extending to the perimeter of a sphere of radius r_L: "region III". The distance of each grid point to each neighboring protein atom is calculated and compared to the sum of the van der Waals radii assigned to the protein atom and the water dipole (1.4 Å). A grid point whose distance is less than this sum for any neighboring atom is deleted. Surrounding region III is the continuum dielectric, "region IV".

Charges are assigned to all protein atoms. Four sets of charges for the Fe, S*, and S_γ atoms have been used:

	DF1	DF2	IONIC	UNIFORM
Fe	–0.05/–0.095	0.411/0.488	2.5/2.25	–0.167/–0.25
S*	–0.27/–0.36	–0.395/–0.539	–2/–2	–0.167/–0.25
S_γ	–0.18/–0.295	–0.516/–0.699	–1/–1	–0.167/–0.25

The first and second numbers are for the oxidized and reduced states of the cluster (total charges –2/–3). DF1 and DF2 are based on X_α (Noodleman et al., 1985) and VSB (Chen et al., 1993; Mouesca et al., 1994) Density Functional calculations, respectively. The "IONIC" and "UNIFORM" charge sets represent extremes with respect to the charge distribution within the cluster. Charges for the atoms of region II are taken from a standard library (Lee et al., 1993) (except in the case of the Fe and S* atoms of a second [Fe-S] cluster when present, whose charges are set to zero). The net charge of each residue is zero. Atomic charges are chosen so that amide C=O, amide NH, $C_\alpha H_\alpha$, and side-chain groups are separately electroneutral (if there is no H_α, C_α and its side chain are together electroneutral). In the specific case of the cysteine ligands whose S_γ atoms lie in region I, C_α, C_β, H_α, and H_β atoms are uncharged. In defining region II, electroneutral groups are not subdivided. Thus, if one or more atoms of an electroneutral group are within region II, the remaining atoms of that group are also retained. As a consequence, the protein comprising region II is uncharged overall.

The electrostatic interaction, v, between the prosthetic group (region I) in either its oxidized or reduced state and the protein atoms (region II), water dipoles (region III), and continuum dielectric (region IV) is evaluated as follows. The Coulombic interaction of region I and region II charges yields $v_{Q\mu}$. The protein atoms of region II are assumed to be polarizable. The charges of atoms in region I induce dipoles in these atoms. These induced dipoles in turn create further polarization. Induced dipoles of atoms in region II are calculated self-consistently, using (isotropic) polarizabilities of 0.5 Å^3 for all H atoms and 1.0 Å^3 for all other atoms. The resulting interaction energy is $v_{Q\alpha}$. Water dipoles positioned at grid points orient in the combined electric field of the charges and induced dipoles of regions I and II and of all other water dipoles. The net dipole moment of each water dipole is given by the Langevin equation, well-known in the classical theory of gaseous dielectric constants. The water dipoles are consequently referred to as Langevin dipoles. The energy resulting from the polarization of the Langevin dipole bath is v_L. Lastly, the polarization of the continuum dielectric of dielectric constant ϵ occupying region IV by the protein charges, protein induced dipoles, and Langevin dipoles contributes an energy v_B, calculated using a Born equation. The total interaction energy, given by

$$v = v_{Q\mu} + v_{Q\alpha} + v_L + v_B$$

is evaluated for oxidized and reduced states of region I. The contribution to the free energy difference of oxidized and reduced states of the protein is approximated by

$$\Delta v = \Delta v_{Q\mu} + \Delta v_{Q\alpha} + \Delta v_L + \Delta v_B$$

[2] The reported potential of the [4Fe-4S] cluster of the [Fe-S] flavoprotein trimethylamine dehydrogenase is an exception (Pace & Stankovich, 1991).

The Langevin dipole grid is divided into two parts: an inner grid of spacing 2 Å and an outer grid of spacing 3 Å. The inner grid radius is 12 Å. In the case of the oxidized state of region I a set of 30 grids, displaced translationally from each other, is sampled in order to determine an optimum grid, which is selected to be that giving the maximum energy υ_L. This optimum grid is used without reoptimization in the case of the reduced state of region I.

As discussed above, all residues are electrically neutral in PDLD calculations. Estimates of upper limits to the contributions to $\Delta\upsilon$ of acidic and basic residues which carry net charges of −1 and +1 due to ionization and protonation, respectively, have been obtained by calculating the additional Coulombic interactions of such charges with the cluster, assuming screening by a dielectric constant whose value is chosen to be 80. In the case of *Pa*Fd and *Av*FdI, both of which contain two [Fe-S] clusters, the second cluster is uncharged in PDLD calculations. Estimates of the contributions to $\Delta\upsilon$ arising from the charges of a second cluster have been obtained by calculating the additional Coulombic interactions of such charges with the primary cluster, again assuming screening by a dielectric constant of 80.

Molecular dynamics (MD) has been applied to the structures obtained by X-ray crystallography using the program ENZYMIX (Lee et al., 1993). MD is limited to atoms lying within a sphere of radius 12 Å centered at the cluster centroid. In addition, MD is constrained by isotropic atomic harmonic potentials whose minima are at the crystallographic atomic positions and whose force constants (k) are 150 kcal/Å^2 for cluster Fe, S*, and S_γ atoms and 0.1 kcal/Å^2 for all other atoms. MD is run for 18 ps at 300 K. PDLD calculations are carried out at 36 MD structures taken at 0.5-ps intervals. The results are averaged to yield MD-averaged values of $\Delta\upsilon$.

All calculations were carried out on a VAX 6320.

RESULTS

Our calculations start from X-ray crystal structures of *Pa*Fd, *Av*FdI, and *Cv*HiPIP and are compared to experimentally determined redox potentials.

*Pa*Fd is a "classical" low-potential ferredoxin (Lovenberg, 1973a,b, 1977; Spiro, 1982; Cammack, 1992a). Isolated in its oxidized state, it is reduced by strong reductants such as sodium dithionite. X-ray crystallography of oxidized *Pa*Fd by (L. H.) Jensen and co-workers at 2.0 Å resolution led to a structure comprising a 54-residue polypeptide binding two $[Fe_4S_4^*Cys_4]$ clusters (Adman et al., 1973, 1976); cysteines 8, 11, 14, 45 and 18, 35, 38, 41 ligate Clusters I and II, respectively. The oxidized [Fe-S] clusters are at the 2– oxidation level (Carter et al., 1972). Identical midpoint potentials of ∼−430 mV were measured for the one-electron reduction of each cluster to the 3– oxidation level (Stombaugh et al., 1976).

Very recently, it has been discovered that *Pa*Fd in fact contains 55 residues and that the portion of the earlier sequence

$$Asn_{21}–Ile_{22}–Ile_{23}–Gln_{24}–Gly_{25}–$$

should be corrected (Backes et al., 1991; Professor E. T. Adman, personal communication, 1991) to

$$Asn_{21}–Cys_{22}–Ile_{23}–Gln_{24}–Glu_{25}–Gly_{26}–$$

Accordingly, the ligands of Clusters I and II are now cysteines 8, 11, 14, 46 and 18, 36, 39, 42, respectively. The structure of *Pa*Fd has been re-refined incorporating this revision of the sequence (Backes et al., 1991). The coordinates of both the original structure and the recently revised structure have been used in this work. The former were obtained from Brookhaven (file 1FDX); the latter (henceforth denoted NEW) were kindly provided by Professor E. T. Adman.

In contrast to *Pa*Fd, the 106-residue *Av*FdI contains two different low-potential [Fe-S] clusters with substantially different redox potentials. Recent studies using X-ray crystallography have shown that *Av*FdI as isolated contains $[Fe_4S_4^*Cys_4]$ and $[Fe_3S_4^*Cys_3]$ clusters (Stout et al., 1988; Stout, 1988,1989; Merritt et al., 1993); cysteines 20, 39, 42, 45 and 8, 16, 49 ligate the $[Fe_4S_4^*Cys_4]$ and $[Fe_3S_4^*Cys_3]$ clusters, respectively. *Av*FdI exhibits two one-electron redox couples with midpoint potentials near −420 and −650 mV (Yoch & Arnon, 1972; Iismaa et al., 1991). As a result of spectroscopic studies of oxidized and dithionite-reduced *Av*FdI [Stephens et al. (1991) and references therein], these potentials can be attributed to the 2–/3– couples of the $[Fe_3S_4^*Cys_3]$ and $[Fe_4S_4^*Cys_4]$ clusters, respectively. The midpoint potential of the $[Fe_3S_4^*Cys_3]$ cluster is substantially pH-dependent (Iismaa et al., 1991), as are the CD and MCD of this cluster in its reduced state (Stephens et al., 1991). To further probe the structural basis of this pH dependence, X-ray crystallography of *Av*FdI has very recently been extended to encompass oxidized and (dithionite-) reduced structures at pH 6 and pH 8 (Stout, 1993) [below and above the pK of 7.8 determined electrochemically (Iismaa et al., 1991)]. The absence of major change in the structure of the $[Fe_3S_4^*Cys_3]$ cluster and its immediate neighborhood has led to the conclusion that the pH-dependent properties originate in direct protonation of the cluster in its reduced state (Shen et al., 1993). In this work, the coordinates of *Av*FdI corresponding to the 1.9-Å resolution oxidized pH 8 structure of (C. D.) Stout (Brookhaven file 4FD1) have been used. The pH dependence of the redox behavior of *Av*FdI will be addressed in future publications focusing on the $[Fe_3S_4^*Cys_3]$ cluster and is not further discussed in this paper.

*Cv*HiPIP is the prototypical HiPIP (Lovenberg, 1973a,b, 1977; Spiro, 1982; Cammack, 1992a). Isolated in its reduced state, it is oxidized by strong oxidants such as ferricyanide. X-ray crystallography of *Cv*HiPIP by Kraut and co-workers yielded a 2.0-Å resolution structure comprising an 85-residue polypeptide binding one $[Fe_4S_4^*Cys_4]$ cluster (Carter et al., 1972, 1974a,b; Freer et al., 1975); cysteines 43, 46, 63, and 77 ligate the cluster. Structures were obtained for both reduced and oxidized HiPIP. The reduced and oxidized clusters are at the 2– and 1– oxidation levels (Carter, 1972). The midpoint potential of the 2–/1– couple is ∼+350 mV (Bartsch, 1963; Mizrahi et al., 1976). Expression of the 2–/3– couple has been sought by a variety of approaches. Cammack (1973) has reported the observation of a "g = 1.94" EPR spectrum, characteristic of $[Fe_4S_4^*Cys_4]^{3-}$ clusters, for *Cv*HiPIP in the presence of DMSO. However, the 3– level has not been detected in the absence of a denaturing agent. The 2–/3– midpoint potential is clearly very low. In this work, the coordinates of oxidized *Cv*HiPIP, obtained from Brookhaven (file 1HIP) have been used. Lys 18, Ser 26, Ala 32, and Gln 50 were incompletely defined and have been modeled in this work as Ala, Ala, Gly, and Ala, respectively.

The values of $\Delta\upsilon$ obtained for *Pa*Fd (Clusters I and II), *Av*FdI, and *Cv*HiPIP using the Brookhaven files 1FDX, 4FD1, and 1HIP, respectively, and the Fe, S*, and S_γ charges of set DF1 are given in Table 1. The protein and Langevin dipole radii r_2 and r_L were both 25 Å. With this value of r_2, no protein atoms are truncated in *Pa*Fd and *Cv*HiPIP and only 4 of 1638 are lost in *Av*FdI. There is therefore no advantage in increasing r_2 and r_L to values greater than 25 Å.

Table 1: PDLD Calculations[a]

	*Pa*Fd (1FDX)		*Pa*Fd (NEW)		*Av*FdI (4FD1)	*Cv*HiPIP (1HIP)
	I	II	I	II		
$\Delta\upsilon_{Q\mu}$	85.2	80.5	91.2	88.6	93.9	33.6
$\Delta\upsilon_{Q\alpha}$	22.3	27.0	21.5	22.9	25.4	50.9
$\Delta\upsilon_L$	51.6	52.0	47.5	44.6	37.5	46.9
$\Delta\upsilon_B$	31.0	30.9	31.0	31.0	31.0	31.1
$\Delta\upsilon$	190.1	190.4	191.2	187.1	187.8	162.5
$\Delta\Delta\upsilon$[b]	2.3	2.6	3.4	−0.7	0	−25.3
$\Delta\mathcal{E}^0$[c]	100	113	147	−30	0	−1097
no. of atoms[d]	737	737	743	743	1634 (1638)	1201
no. of Langevin dipoles	2443	2448	2400	2425	2151	2208
no. of Langevin dipoles <6 Å	4	7	4	5	0	5

[a] All calculations use $r_2 = r_L = 25$ Å; carry out 10 iterations in calculating $\Delta\upsilon_{Q\alpha}$; select the optimum grid from 30 options; and carry out 30 iterations in calculating $\Delta\upsilon_L$. Energies are in kcal/mol. [b] $\Delta\Delta\upsilon = \Delta\upsilon - \Delta\upsilon$ (*Av*FdI). [c] $\Delta\mathcal{E}^0$ is the calculated redox potential difference from *Av*FdI in mV: $[\Delta\Delta\upsilon$ (kcal/mol)$]/(23.06 \times 10^{-3})$. [d] Number of protein atoms in region II; total number in parentheses where different.

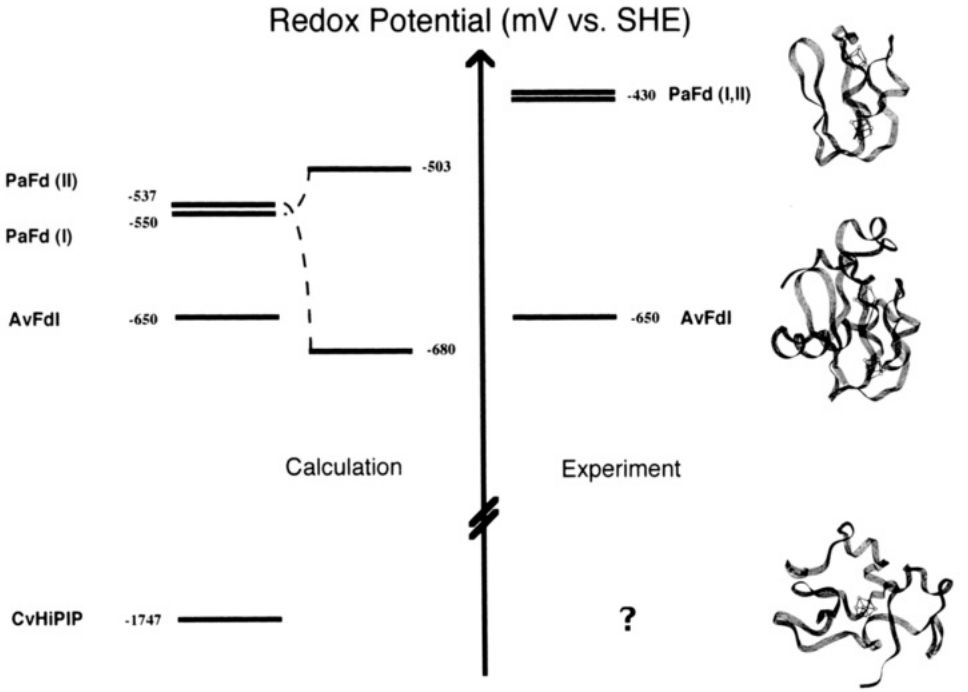

FIGURE 1: Calculated and experimental redox potentials of *Pa*Fd, *Av*FdI, and *Cv*HiPIP. Calculated and experimental potentials of *Av*FdI are arbitrarily set equal. Left-hand and right-hand calculations for *Pa*Fd are for coordinates 1FDX and NEW, respectively.

The values of $\Delta\upsilon$ in Table 1 predict the differences in redox potentials of the $[Fe_4S_4^*Cys_4]^{2-/3-}$ couples of *Pa*Fd (Clusters I and II), *Av*FdI, and *Cv*HiPIP. The potentials of Clusters I and II of *Pa*Fd are predicted to lie 100 and 113 mV higher than that of *Av*FdI, while the potential of *Cv*HiPIP is predicted to lie 1097 mV lower. Fixing (arbitrarily)[3] the intrinsic redox potential to be such that the redox potential of *Av*FdI, including the calculated protein and water contributions, is equal to the experimental value of −650 mV, the predicted potentials of *Pa*Fd and *Cv*HiPIP are −550 mV (*Pa*Fd, Cluster I), −537 mV (*Pa*Fd, Cluster II), and −1747 mV (*Cv*HiPIP). As illustrated in Figure 1, these results are in qualitative agreement with experiment in predicting that the potentials of Clusters I and II of *Pa*Fd are very similar, and higher than that of *Av*FdI. In addition, the enormously lower potential predicted for *Cv*HiPIP is consistent with the undetectability (to date) of this couple. Quantitatively, the predicted difference in potentials of Clusters I and II of *Pa*Fd, 13 mV, is in excellent agreement with the experimental value, 0 mV. The differences in potential from *Av*FdI, 100 and 113 mV for Clusters I and II, compare to the experimental value of 220 mV for both clusters.

Our calculations for *Pa*Fd have been repeated using coordinates (NEW) obtained by refinement of a structure incorporating the corrected sequence against the original (2.0-Å) data. The results are given in Table 1 and Figure 1. The predicted potentials of Clusters I and II change by +47 and −143 mV, respectively. A greater change in $\Delta\upsilon$ for Cluster II than for Cluster I is to be expected since the structural changes are greater in the vicinity of Cluster II. The difference in potentials of Clusters I and II changes from −13 to +177 mV. The difference in potential from that of *Av*FdI changes from 100 to 147 mV and from 113 to −30 mV for Clusters I and II, respectively. The difference in potentials of Clusters I and II is in much worse agreement with experiment. The difference in potential from *Av*FdI is in improved agreement with experiment for Cluster I and in significantly worse agreement for Cluster II.

The calculations for *Pa*Fd using the NEW coordinates and for *Av*FdI have been repeated using three alternative sets of

[3] In principle, the intrinsic redox potential could be obtained from the experimental redox potential of the naked prosthetic group in water. In this case, this potential is not known. Calculated values of $\Delta\upsilon$ for the $[Fe_4S_4^*(S_\gamma)_4]^{2-/3-}$ clusters of *Pa*Fd, *Av*FdI, and *Cv*HiPIP are 168–171 kcal/mol (using the calculational parameters of Table 1), 700–1000 mV lower than the calculated $\Delta\upsilon$ for *Av*FdI and *Pa*Fd.

Table 2: Variation of Cluster Charges[a,b]

	*Pa*Fd (NEW)								*Av*FdI			
	I				II							
	DF1	DF2	I	U	DF1	DF2	I	U	DF1	DF2	I	U
$\Delta\upsilon_{Q\mu}$	91.2	89.1	94.7	91.6	88.6	86.3	92.3	89.0	93.9	92.7	95.9	93.8
$\Delta\upsilon_{Q\alpha}$	21.5	15.7	4.1	22.6	22.9	17.1	7.2	24.1	25.4	18.9	7.5	26.7
$\Delta\upsilon_L$	47.5	47.6	47.4	47.5	44.6	45.4	43.0	44.7	37.5	38.6	38.0	37.5
$\Delta\upsilon_B$	31.0	31.0	31.0	30.9	31.0	30.9	30.9	30.9	31.0	31.0	31.0	30.9
$\Delta\upsilon$	191.2	183.4	177.2	192.6	187.1	179.7	173.4	188.7	187.8	181.2	172.4	188.9
$\Delta\Delta\upsilon$	3.4	2.2	4.8	3.7	−0.7	−1.5	+1.0	−0.2	0	0	0	0
$\Delta\mathscr{E}^0$	147	95	208	160	−30	−65	+43	−9	0	0	0	0

[a] Definitions, units, and calculational parameters as in Table 1. [b] I and U are the alternative charge sets IONIC and UNIFORM (see text).

Table 3: Variation of H Atom Positions[a]

	*Pa*Fd (NEW)		*Av*FdI
	I	II	
$\Delta\upsilon_{Q\mu}$	92.3	93.8	94.1
$\Delta\upsilon_{Q\alpha}$	21.2	21.2	25.5
$\Delta\upsilon_L$	50.2	40.8	37.2
$\Delta\upsilon_B$	30.9	30.9	31.0
$\Delta\upsilon$	194.6	186.7	187.8
$\Delta\Delta\upsilon$	6.8	−1.1	0
$\Delta\mathscr{E}^0$	295	−48	0

[a] Definitions, units, and calculational parameters as in Table 1.

Table 4: Net Charge Contributions [a]

	*Pa*Fd (NEW)		*Av*FdI	*Cv*HiPIP
	I	II		
$\Delta\upsilon^b$	−1.8	−2.3	−5.2	0.6
$\Delta\Delta\upsilon^b$	+3.4	+2.9	0	+5.8
$\Delta\mathscr{E}^{0\,b}$	147	126	0	252
$\Delta\upsilon^c$	−0.7	−1.5	−3.6	
$\Delta\Delta\upsilon^c$	+2.9	+2.1	0	
$\Delta\mathscr{E}^{0\,c}$	126	91	0	

[a] Definitions, units, and calculational parameters as in Table 1. [b] All acidic and basic residues included. [c] Only acidic and basic residues within 10 Å of the cluster included. For *Pa*Fd(I) these are Asp 6, Glu 17 and 25, and Lys 15; for *Pa*Fd(II) they are Asp 32, 34, and 38, Glu 17, and Lys 15; for *Av*FdI they are Asp 23 and 41 and Glu 18, 38, 46, and 48.

Fe, S*, and S_γ charges: DF2, IONIC, and UNIFORM, with the results given in Table 2. As expected, $\Delta\upsilon$ is sensitive to the choice of charges. However, the differences in $\Delta\upsilon$ are much less sensitive; relative to *Av*FdI, $\Delta\upsilon$ for Clusters I and II of *Pa*Fd varies only 2.6 and 2.5 kcal/mol, respectively, equivalent to 113 and 108 mV. The differences in potential between Clusters I and II of *Pa*Fd and between Cluster II of *Pa*Fd and *Av*FdI are not significantly improved in their agreement with experiment by any alternative choice of charges.

The POLARIS program adds H atoms to the "heavy atom" structure obtained by X-ray crystallography. In the case of H atoms likely to exhibit conformational flexibility, dihedral angles are given "standard" values. The consequences of rotations of such H atoms have been examined for *Pa*Fd and *Av*FdI. H atoms attached to the O, S, and N atoms of all Ser, Thr, Tyr, Cys, Lys, and Arg residues have been rotated through 360° and relative energies calculated at selected angles *via* a simple electrostatic algorithm. $\Delta\upsilon$ has then been recalculated with all H atoms at their minimum energy positions. The results are given in Table 3. Neither relative nor absolute changes in $\Delta\upsilon$ are large. The predicted difference in potential between Clusters I and II of *Pa*Fd is increased and is in worse agreement with experiment. The predicted difference in potential between Cluster I of *Pa*Fd and *Av*FdI is increased and is in comparable agreement with experiment. The predicted difference in potential between Cluster II of *Pa*Fd and *Av*FdI is very little changed and remains in poor agreement with experiment.

*Pa*Fd, *Av*FdI, and *Cv*HiPIP contain relatively large numbers of acidic residues, as well as some basic residues. Upper limits to the contributions of net charges on these residues to cluster redox potentials have been estimated by assuming net charges of −1 and +1 on acidic and basic residues, respectively, and using a macroscopic dielectric constant of 80. The results obtained are given in Table 4. The corresponding values obtained including only those residues within 10 Å of the cluster centroid are also given in Table 4. The greater number of acidic residues in *Av*FdI than in *Pa*Fd increases the potentials of Clusters I and II relative to *Av*FdI. The changes are similar for Clusters I and II. Smaller changes are predicted when the residues included are limited to those within 10 Å. These calculated contributions are upper limits to the actual contributions at near-physiological pHs since interactions between charged residues lead to shifts in p*K* which in turn decrease the net charges on these residues. It thus appears that, while small increases in the potentials of Clusters I and II relative to *Av*FdI may result from net charges, the magnitude of these effects is small. Furthermore, their inclusion does not bring the predicted potentials of Clusters I and II of *Pa*Fd closer together.

In the cases of *Pa*Fd and *Av*FdI, the contribution of the charge of the second [Fe-S] cluster has been similarly estimated. For Clusters I and II of *Pa*Fd the contributions are −1.1 or −0.7 kcal/mol (48 or 30 mV), assuming the second cluster to be at the −3 or −2 oxidation level respectively. For *Av*FdI the contribution of the $[Fe_3S_4^*Cys_3]$ cluster in the 3− oxidation level is −1.1 kcal/mol (48 mV). Relative to *Av*FdI, the potentials of Clusters I and II are shifted by 0 or +18 mV. Cluster-cluster interaction can thus be ignored.

Molecular dynamics (MD) has also been applied to *Pa*Fd, *Av*FdI, and *Cv*HiPIP, and MD averages of PDLD results obtained. Constrained MD was carried out with clusters in the 2− (oxidized) oxidation level. In the case of *Pa*Fd, the coordinates NEW constituted the starting point for MD. $\Delta\upsilon$ values calculated at 0.5 ps intervals are shown in Figure 2. Averages are given in Table 5. The difference in potential calculated for Clusters I and II of *Pa*Fd is reduced to 56 mV and is in improved agreement with experiment. However, the differences in potential from *Av*FdI are >500 mV, in worse agreement with experiment, especially for Cluster I.

DISCUSSION

The results obtained using the PDLD model for the $[Fe_4S_4^*Cys_4]$ clusters of *Pa*Fd, *Av*FdI, and *Cv*HiPIP raise a variety of specific questions, answers to which not only deepen our understanding of the redox potentials of these three proteins

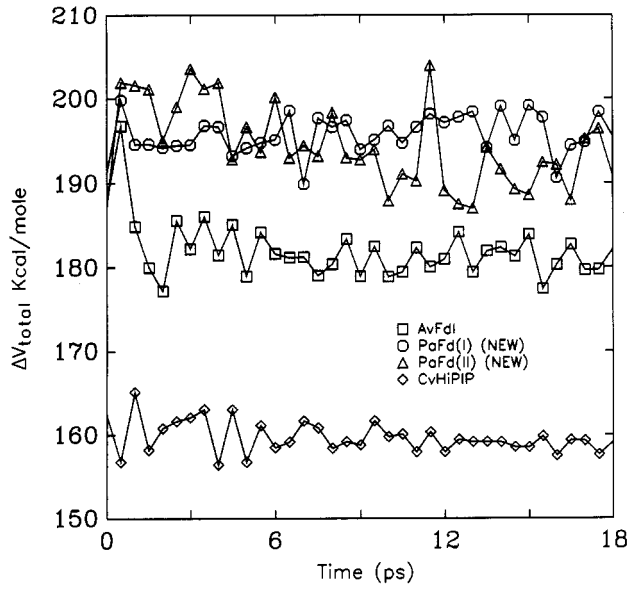

FIGURE 2: Variation of calculated values of Δv over 18 ps of molecular dynamics.

Table 5: Molecular Dynamics [a,b]

	*Pa*Fd (NEW)		*Av*FdI
	I	II	
$\Delta v_{Q\mu}$	99.1	104.6	90.8
$\Delta v_{Q\alpha}$	22.2	22.0	30.0
Δv_L	43.6	37.0	30.6
Δv_B	31.0	31.0	31.1
Δv	195.9	194.6	182.5
$\Delta\Delta v$	13.4	12.1	0
$\Delta\mathcal{E}^0$	581	525	0

[a] Definitions, units, and calculational parameters as in Table 1. [b] Results are averages of 36 steps of molecular dynamics (see text).

but also illuminate the factors of general importance in determining the redox potentials of [Fe-S] proteins.

Is the Redox Potential of the 2-/3- Couple of an [$Fe_4S_4^*Cys_4$] Cluster Determined by Its Local Environment or Is the Entire Protein Structure of Importance? Calculations as a function of r_2 answer this question. Results with r_L = 25 Å are diagrammed in Figure 3. In each case, as r_2 – and therefore, the number of protein atoms in region II – increases, ($\Delta v_{Q\mu} + \Delta v_{Q\alpha}$) and Δv_L progressively increase and decrease, respectively. The total Δv converges to a plateau by r_2 = 15–18 Å. It is of minor importance whether beyond 15 Å or so there is protein or water. The large differences in Δv between the clusters of *Pa*Fd and *Av*FdI on the one hand and *Cv*HiPIP on the other are already developed at r_2 = 6 Å. However, the small differences in Δv among the clusters of *Pa*Fd and *Av*FdI fluctuate considerably (and irregularly) over the range r_2 = 6–15 Å. Thus, it can be concluded that the immediate environment of the cluster is of predominant importance and dictates the range in which its redox potential lies. At the same time, protein shells beyond that immediately surrounding the cluster are of importance in determining the smaller variations among clusters whose redox potentials lie in the same range.

Of the Many Charges (Dipoles) Surrounding Each [$Fe_4S_4^*Cys_4$] Cluster in PaFd, AvFdI, and CvHiPIP, Which Are of Especial Importance? The contributions of the charges of each residue to $\Delta v_{Q\mu}$ for each cluster are plotted in Figure 4 (with the exception of residues 67–106 of *Av*FdI). Values lie in the range –5 to +10 kcal/mol. The separate contributions of the main-chain amide and $C_\alpha H_\alpha$/side-chain moieties of each residue are also displayed in Figure 4. It is immediately apparent that all large contributions arise from amide groups, while the contributions of the $C_\alpha H_\alpha$ and side-chain groups are larger than 2 kcal/mol in only one case and are thus relatively insignificant.

In Table 6 we list the amide groups whose individual contributions to $\Delta v_{Q\mu}$ exceed 4.0 kcal/mol, together with the magnitude of the contribution and the distances of the amide N and O atoms to the cluster centroid. The variation in $\Delta v_{Q\mu}$ with r_2 exhibited in Figure 3 leads to the expectation that groups making outstanding contributions to $\Delta v_{Q\mu}$ are already included in calculations at r_2 = 6 Å. Table 6 confirms this expectation. In the case of Clusters I and II of *Pa*Fd and of *Av*FdI 13 amide groups contribute > 4 kcal/mol to $\Delta v_{Q\mu}$. In *Cv*HiPIP there are 7 such amide groups. As a result of the approximate 2-fold symmetry of *Pa*Fd, the environments of its two clusters exhibit strong structural homology. Further, the environments of the *Pa*Fd clusters also exhibit strong homology with that of the [$Fe_4S_4^*Cys_4$] cluster of *Av*FdI. In Table 6, the amide group contributions of *Pa*Fd and *Av*FdI have been ordered so as to align homologous amide groups. In almost all cases, contributions of homologous amides are either all >4 kcal/mol or all <4 kcal/mol. In a very few cases, the contribution for one cluster is >4 kcal/mol and for the other two clusters is <4 kcal/mol. In these cases, the latter contributions have also been included in Table 6 for completeness. Thus, for *Pa*Fd and *Av*FdI there result in the end 15 important amide groups. Nearly all—but not all—of these contributions to $\Delta v_{Q\mu}$ are positive, indicating that in nearly all amides the positive end of the amide dipole is closer to the cluster than the negative end. Examination of the distances of the amide N and O atoms from the cluster centroid (Table 6) confirms this conclusion. The 15 "especially important" amide groups in *Pa*Fd and *Av*FdI and the 7 such groups in *Cv*HiPIP are shown in pictorial form in Figure 5.

The sums of the amide group contributions to $\Delta v_{Q\mu}$ listed in Table 6 are 84.3, 83.2, 79.1, and 32.0 for *Pa*Fd Cluster I, *Pa*Fd Cluster II, *Av*FdI, and *Cv*HiPIP, respectively. The total $\Delta v_{Q\mu}$ values (Table 1) are 91.2, 88.6, 93.9, and 33.6 kcal/mol. Clearly, in each protein an overwhelming fraction of the total $\Delta v_{Q\mu}$ originates in a very small number of amide groups. The importance of the charges (dipoles) of amide groups in general and of the "especially important" amide groups identified in Table 6 in particular to the overall Δv can be evaluated by calculations in which these charges are deleted, with the results given in Table 7. The cancellation of protein charges (dipoles) leads not only to a decrease in $\Delta v_{Q\mu}$ but also to a compensating increase in $\Delta v_{Q\alpha}$ and Δv_L. In the case of *Pa*Fd and *Av*FdI, deletion of the amide group charges causes very large decreases in total Δv and potential; in contrast, in the case of *Cv*HiPIP the net changes are very small. Thus, in the absence of the charges (dipoles) of the "especially important" amide groups in *Pa*Fd, *Av*FdI, and *Cv*HiPIP their potentials would be much more nearly equal, and those of *Pa*Fd and *Av*FdI would be in a very different, much lower, range.

While the major part of $\Delta v_{Q\mu}$ in *Pa*Fd, *Av*FdI, and *Cv*HiPIP originates in the charges (dipoles) of the "especially important" amide groups, the charges of other amide groups and of $C_\alpha H_\alpha$ and side-chain groups cannot be ignored. The values of Δv and $\mathcal{E}^0$ predicted without these latter charges are also given in Table 7. For *Pa*Fd Cluster I, *Pa*Fd Cluster II, *Av*FdI, and *Cv*HiPIP the differences from calculations including all charges are 3.6 (156), 2.1 (91), 1.1 (48), and 4.6 (199)

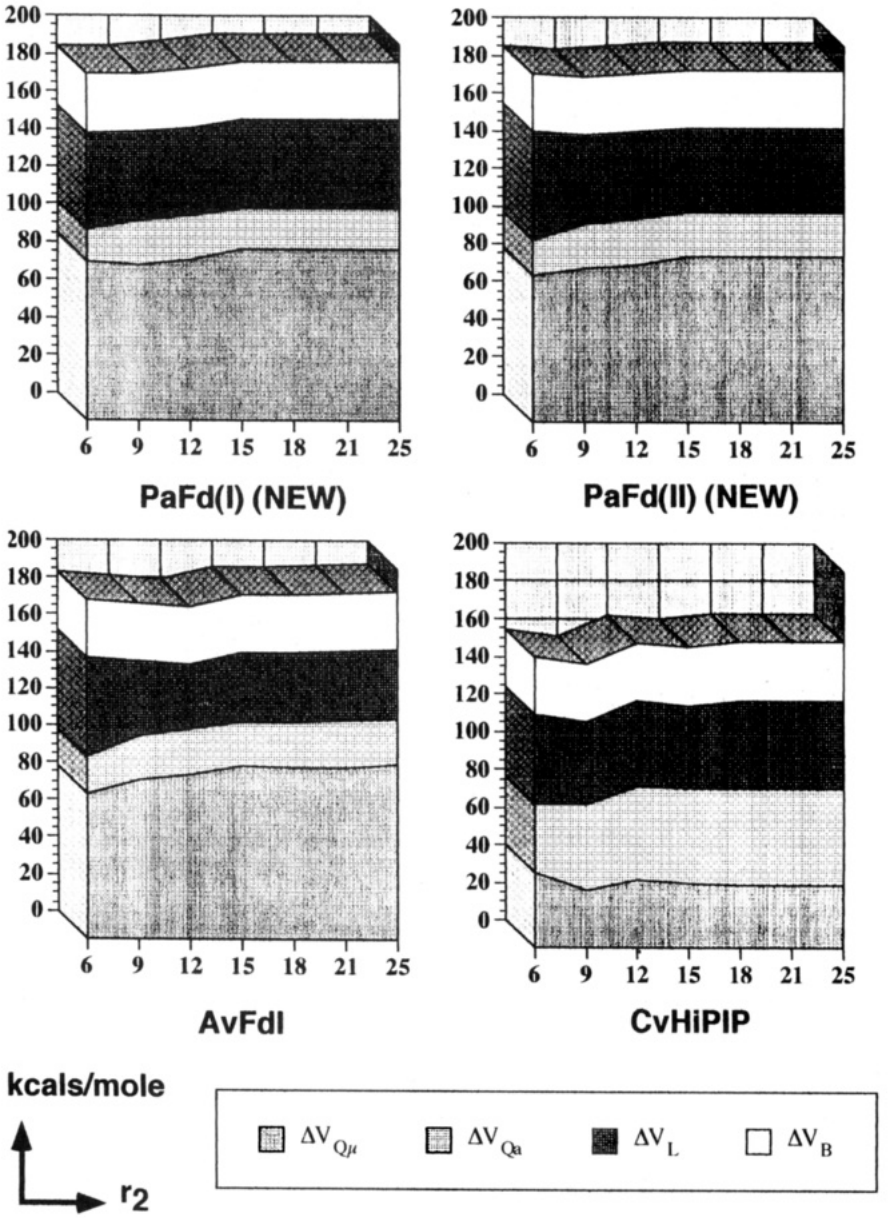

FIGURE 3: Variation of calculated values of $\Delta\upsilon_{Q\mu}$, $\Delta\upsilon_{Q\alpha}$, $\Delta\upsilon_L$, $\Delta\upsilon_B$, and $\Delta\upsilon$ as a function of r_2. r_2 was varied from 6 to 25 Å in steps of 3 Å. Other calculational parameters as in Table 1.

kcal/mol (mV), respectively. Similar calculations including the charges of all amide groups lead to comparable deviations: 4.5 (195), 0.4 (17), 1.8 (78), and 2.7 (117) kcal/mol (mV). Thus, the contributions of the charges (dipoles) of the other amide groups and of the $C_\alpha H_\alpha$ and side-chain groups are overall comparable in magnitude.

Are Langevin Dipoles (Water Molecules) Close to the [$Fe_4S_4^*Cys_4$] Cluster, and If So, Are They of Particular Significance? The number of Langevin dipoles within a sphere of radius r centered at the cluster centroid as a function of r is shown in Figure 6 for *Pa*Fd (Cluster I) and *Av*FdI. The contribution to $\Delta\upsilon_L$ of Langevin dipoles within a sphere of radius r as a function of r is also shown in Figure 6. Within a sphere of radius 25 Å the number of Langevin dipoles is 2400 and 2151 for *Pa*Fd and *Av*FdI, respectively. The values of $\Delta\upsilon_L$ are 47.5 and 37.5 kcal/mol, tracking the number of dipoles, as expected. The average per dipole contribution to $\Delta\upsilon_L$ is ~0.02 kcal/mol. Within a sphere of radius 6 Å there are 4 and 0 dipoles in *Pa*Fd and *Av*FdI, respectively. The contribution to $\Delta\upsilon_L$ of the 4 dipoles in *Pa*Fd is 6.0 kcal/mol, corresponding to a 1.5 kcal/mol average contribution per dipole. Clearly, these "local" dipoles are particularly important contributors to $\Delta\upsilon_L$ in *Pa*Fd. Of the total $\Delta\upsilon_L$ at r = 25 Å, 47.5kcal/mol, they contribute 13%. If their contribution to $\Delta\upsilon_L$ were subtracted, $\Delta\upsilon$ would be 185.2 kcal/mol, lower than that predicted for *Av*FdI. The locations of the 4 Langevin dipoles within r = 6 Å of Cluster I of *Pa*Fd are illustrated pictorially in Figure 7. For each dipole, the protein atoms immediately adjacent are detailed in the caption.

Water molecules are included in the refined X-ray structures of *Pa*Fd and *Av*FdI. In the case of *Pa*Fd, the original structure (Adman et al., 1976) contained 146 water molecules. Unfortunately, their coordinates are not in the Brookhaven file 1FDX. The revised structure (coordinates NEW) contains 95 water molecules; none are within 6 Å of the center of Cluster I. In the case of *Av*FdI, the 1.9-Å resolution pH 8.0 structure of oxidized *Av*FdI reported by Stout (1989) (4FD1) incorporates 21 water molecules. The structure of oxidized *Av*FdI at pH 6.0 more recently reported by Stout (1993) retains 20 of the 21 molecules found at pH 8.0. In the 2.3-Å resolution pH 6.5 structure of oxidized *Av*FdI reported by Merritt et al. (1993) there are 98 water molecules, 20 of which are identically

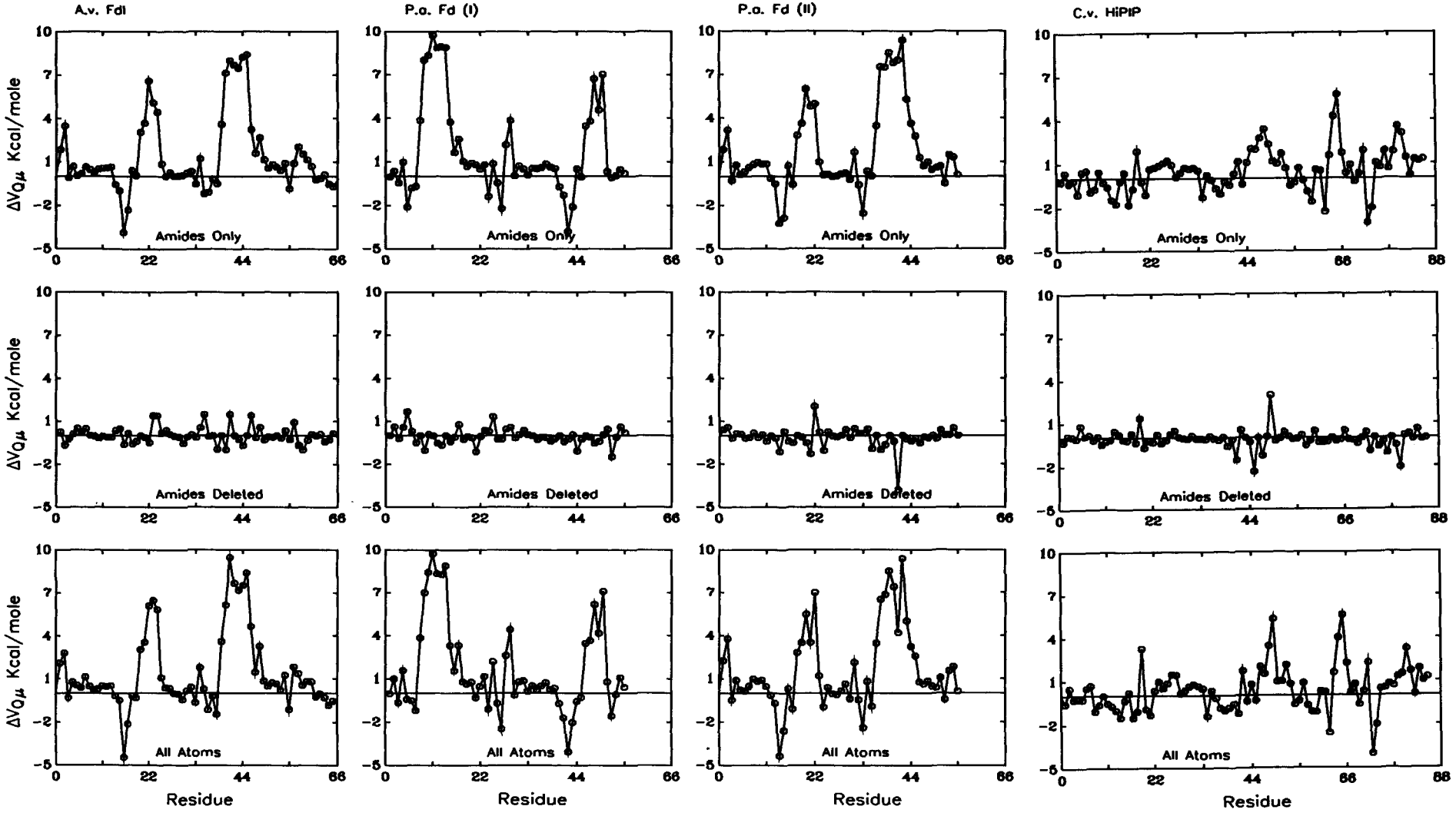

FIGURE 4: Contributions of individual residues to $\Delta v_{Q\mu}$. Upper panel: charges on main-chain amide groups only; middle panel: charges on $C_\alpha H_\alpha$ and side-chain groups only; bottom panel: all charges included.

Table 6: Amide Group Contributions to Δv_{Q_μ}

*Pa*Fd(I)						*Av*FdI						*Pa*Fd(II)						*Cv*HiPIP					
amide N[a]	Δv_{Q_μ}[b]	r_N[c]	r_O[d]	S[e]	r_{NS}[f]	amide N[a]	Δv_{Q_μ}[b]	r_N[c]	r_O[d]	S[e]	r_{NS}[f]	amide N[a]	Δv_{Q_μ}[b]	r_N[c]	r_O[d]	S[e]	r_{NS}[f]	amide N[a]	Δv_{Q_μ}[b]	r_N[c]	r_O[d]	S[e]	r_{NS}[f]
29*	7.4	6.4	8.6	S_γ8	3.4	2	6.7	6.3	8.3	S*3	3.4	2*	6.9	6.4	8.6	S_γ36	3.5	20	3.9	8.4	9.6	S_γ77	6.9
43	–4.2	8.3	6.5	S_γ46	6.7	17	–4.6	8.6	6.8	S_γ20	7.0	15	–4.0	8.8	7.1	S_γ18	7.1	48*	4.9	6.2	8.2	S_γ46	3.7
47	4.6	5.8	7.0	S_γ46	3.5	21	4.7	5.7	6.9	S_γ20	3.7	19	4.4	5.8	7.0	S_γ18	3.6	64	4.3	6.9	7.6	S_γ63	3.3
48*	8.0	6.4	8.4	S_γ46	3.4	22	7.6	6.4	8.4	S_γ20	3.6	20*	7.3	6.6	8.6	S_γ18	3.9	65*	6.8	7.0	9.2	S_γ63	3.5
49	3.8	7.2	8.0	S_γ46	3.4	23	4.5	7.2	8.3	S_γ20	3.4	21	3.8	7.2	8.2	S_γ18	3.5	73	–5.1	8.9	7.2	S_γ43	5.4
50*	7.1	6.3	8.6	S_γ46	3.4	24	7.0	6.7	8.9	S_γ20	3.6	22*	7.3	6.6	8.8	S_γ18	3.4	77*	4.5	5.1	6.2	S_γ77	3.6
6	–4.0	9.9	7.8	S_γ8	7.3	36	–2.0	9.6	8.0	S_γ39	6.6	33	–3.0	9.1	7.8	S_γ36	6.5					S*1	3.7
9*	9.3	5.1	6.8	S_γ8	3.4	40	8.5	5.2	6.8	S*1	3.5	37*	8.7	5.2	6.8	S*68	3.5	79*	5.6	6.4	8.4	S_γ77	3.5
				S*61	3.3					S_γ39	3.5					S_γ36	3.5	81*	7.0	6.6	7.6	S_γ46	3.7
10*	7.5	5.1	6.8	S_γ8	3.4	41	7.0	5.1	6.7	S_γ39	3.3	38*	6.8	5.2	6.8	S_γ36	3.6						
11	9.0	4.7	6.6	S_γ11	3.3	42	7.7	4.8	6.6	S_γ42	3.3	39	8.5	4.9	6.8	S_γ39	3.4						
				S*60	3.7					S*2	3.6					S*71	3.7						
12*	10.3	4.8	6.8	S_γ11	3.2	43	7.8	4.9	6.5	S*2	3.2	40*	8.2	4.9	6.6	S*71	3.4						
				S*60	3.4					S_γ42	3.4					S_γ39	3.4						
13*	8.2	5.1	6.6	S_γ11	3.4	44	7.9	5.2	6.7	S_γ42	3.4	41*	7.1	5.2	6.7	S_γ39	3.5						
14*	9.5	5.0	7.1	S_γ14	3.1	45	9.0	5.1	7.2	S_γ45	3.1	42*	8.0	5.0	7.1	S_γ42	3.0						
				S*63	3.5					S*4	3.7					S*70	3.4						
15	6.5	6.8	7.7	S_γ14	3.3	46	5.4	6.8	7.7	S_γ45	3.4	43	9.7	6.6	7.7	S_γ42	3.2						
16	1.9	9.5	10.2	S_γ14	6.3	47	1.8	9.6	10.3	S_γ45	6.4	44	4.1	8.6	10.0	S_γ42	5.8						

[a] Residue number. Amides defined as H-bonding to cluster S atoms by Backes et al. (1991) are asterisked. [b] kcal/mol. [c] Distance of amide N to $[Fe_4S_4^*(S_\gamma)_4]$ centroid (Å). [d] Distance of amide O to $[Fe_4S_4^*(S_\gamma)_4]$ centroid (Å). [e] Cluster S atoms ≤4 Å from amide N. [f] Distance of cluster S from amide N (Å).

Table 7: Charge Deletions

	*Pa*Fd(I)					*Av*FdI					*Pa*Fd(II)					*Cv*HiPIP				
	a	*b*	*c*	*d*	*e*	*a*	*b*	*c*	*d*	*e*	*a*	*b*	*c*	*d*	*e*	*a*	*b*	*c*	*d*	*e*
Δv_{Q_μ}	–2.6	6.9	84.3	93.7	91.2	2.9	14.8	79.1	91.0	93.9	–8.3	5.4	83.2	96.8	88.6	–8.6	0.8	32.0	42.2	33.6
Δv_{Q_α}	60.3	54.0	26.0	19.7	21.5	65.6	58.0	32.0	24.4	25.4	64.2	56.4	25.1	17.3	22.9	72.0	66.8	51.5	46.1	50.9
Δv_L	57.4	58.3	46.4	51.4	47.5	46.5	45.4	44.7	39.6	37.5	52.0	56.8	45.7	41.7	44.6	52.1	48.0	43.4	45.9	46.9
Δv_B	31.1	31.0	30.9	30.9	31.0	31.0	31.0	30.9	31.0	31.0	31.1	31.0	31.0	30.9	31.0	31.0	31.2	31.0	31.0	31.1
Δv	146.2	150.2	187.6	195.7	191.2	146.0	149.2	186.7	186.0	187.8	139.0	149.6	185.0	186.7	187.1	146.5	146.8	157.9	165.2	162.5
$\Delta\Delta v$	0.2	1.0	0.9	9.7	3.4	0	0	0	0	0	–7.0	0.4	–1.7	0.7	–0.7	0.5	–2.4	–28.8	–20.8	–25.3
ΔG^0	9	43	39	421	147	0	0	0	0	0	–304	17	–74	30	–30	22	–104	–1249	–902	–1097

[a] All amide group charges deleted. [b] "Especially important" amide group charges deleted. [c] "Especially important" amide group charges included; all other charges deleted. [d] All amide group charges included; all other charges deleted. [e] All charges included (see Table 1).

located to those identified by Stout in the pH 8.0 and 6.0 structures. In no structure are water molecules within 6 Å of the cluster centroid. Thus, our calculations are consistent with the available X-ray analyses of *Av*FdI in finding no water molecules very close to the $[Fe_4S_4^*Cys_4]$ cluster. On the other hand, our calculations have placed water molecules within 6 Å of the centroid of Cluster I of *Pa*Fd while such molecules are not present in the solvent model reported for *Pa*Fd. It is possible that further study of *Pa*Fd by X-ray crystallography will lead to the detection of such "local" water molecules. It is possible that such molecules exist but are not detectable by X-ray methods. It is possible that our calculations erroneously insert "local" dipoles at locations which in fact do not support water molecules. These possibilities can only be distinguished by further X-ray work and by calculations incorporating more sophisticated and reliable solvent models.

Why Are the Differences in Potential of Cluster II of PaFd from Those of Cluster I and of AvFdI Inadequately Predicted by the Revised (NEW) Coordinates for PaFd? Three possibilities exist: (1) inadequacy of the PDLD model; (2) error in the X-ray coordinates; (3) disorder/conformational multiplicity in the vicinity of Cluster II of *Pa*Fd. We have shown that the potentials of Clusters I and II can be much more nearly equalized by using an ensemble of structures generated from the X-ray coordinates of *Pa*Fd by means of molecular dynamics (MD). This points to either the second or third possibilities – or both – as the most likely source of the Cluster II problem. The variation in Δv resulting from the MD is greater for Cluster II than for Cluster I, possibly indicating greater flexibility around the former cluster. Further study of the structure and dynamics of *Pa*Fd in the vicinity of Cluster II will clearly be of interest.

Our calculations have demonstrated the pre-eminent importance of the number and – especially – the orientation of the amide groups in the neighborhood of a $[Fe_4S_4^*Cys_4]$ cluster in determining its redox potential. Thus, to a first approximation, the folding of the protein backbone determines the range in which the redox potentials of [Fe-S] proteins are expressed. In the cases of *Pa*Fd, *Av*FdI, and *Cv*HiPIP, the similarity of the potentials of the clusters of *Pa*Fd and *Av*FdI and the relatively enormous difference in potential of the cluster of *Cv*HiPIP are directly attributable to the similarity and difference, respectively, of the folding of these proteins. Proteins whose backbone folding around a $[Fe_4S_4^*Cys_4]$ cluster is similar to that in *Pa*Fd and *Av*FdI should exhibit potentials in the same general range; when the folding is similar to that in *Cv*HiPIP, the potential can be expected to be close to that of *Cv*HiPIP. Proteins possessing qualitatively different folding from *Pa*Fd, *Av*FdI, or *Cv*HiPIP could tune the potentials of their $[Fe_4S_4^*Cys_4]^{2-/3-}$ clusters into substantially different ranges. An increase in the number of favorably oriented local amide groups beyond that in *Pa*Fd and *Av*FdI should lead to yet higher potentials. Conversely, a decrease should lead to lower potentials. Either would appear to be entirely within the bounds of practicability. Obviously, protein

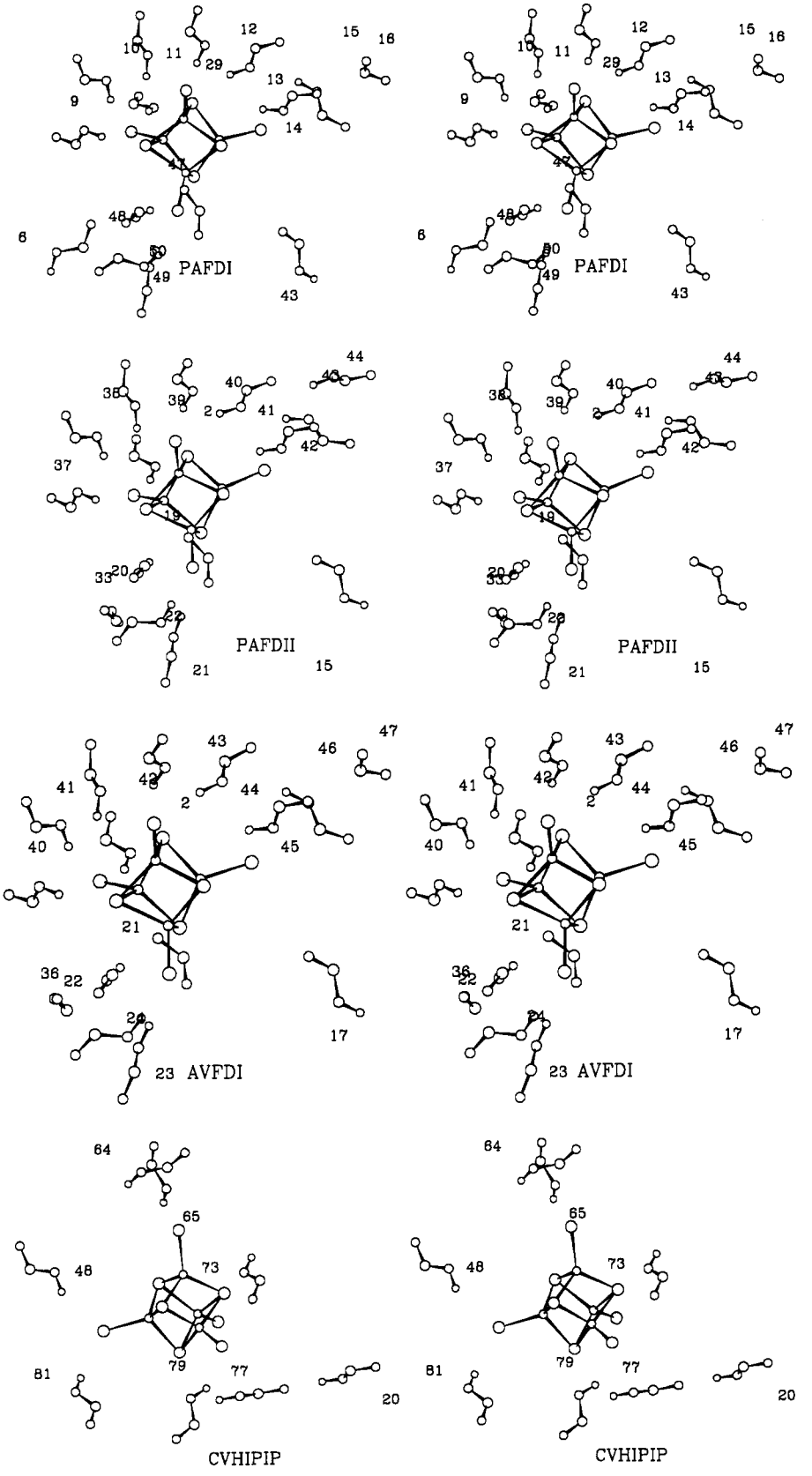

FIGURE 5: Stereodiagrams of the especially important amide groups (as defined in Table 6). Shown are the $[Fe_4S_4^*(S\gamma)_4]$ cluster and the H, N, C, and O atoms of the amide groups.

folding must place four cysteine S_γ atoms suitably in order that a $[Fe_4S_4^*Cys_4]$ cluster exist at all, and this substantially constrains the protein sequences which can express a $[Fe_4S_4^*Cys_4]$ cluster. However, within the subset for which this is possible, there must exist a substantial variety of cluster environments. It will be surprising if the range of measured potentials of 2−/3− couples of $[Fe_4S_4^*Cys_4]$ clusters is not substantially enlarged in the future as more proteins, natural and synthetic, are characterized. In particular, it can be expected that mutant forms of *Pa*Fd and *Av*FdI in which

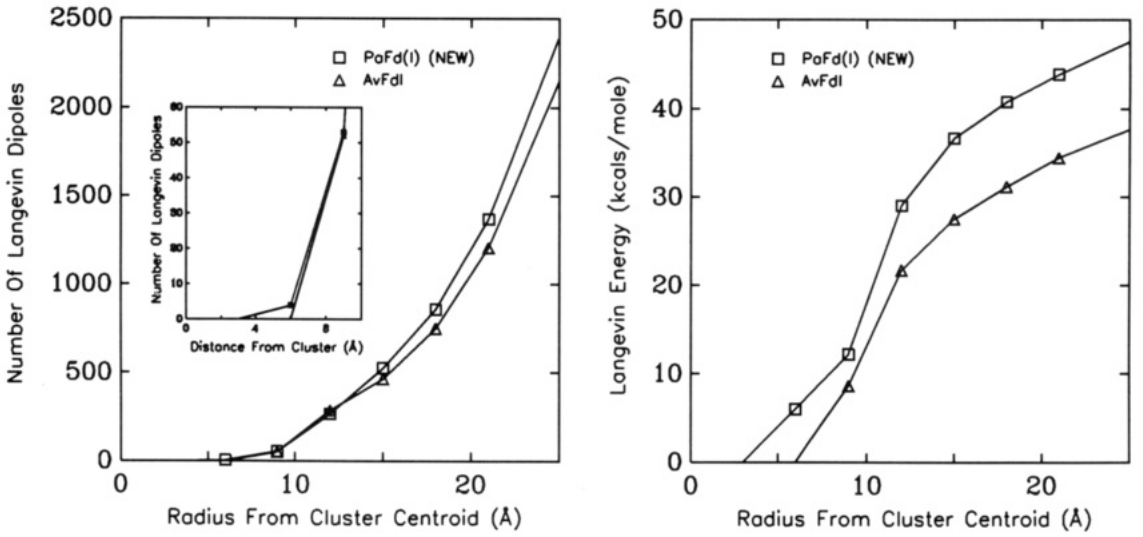

FIGURE 6: Radial distribution of the numbers (left-hand panel) and contributions to $\Delta\upsilon_L$ (right-hand panel) of Langevin dipoles for Cluster I of *Pa*Fd and for *Av*FdI.

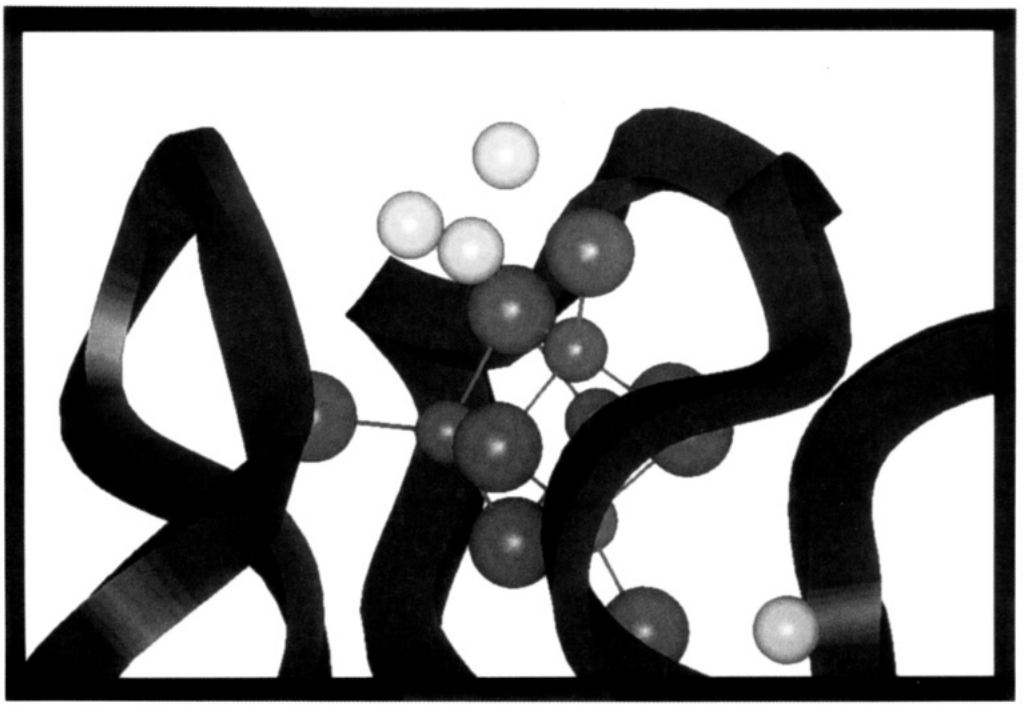

FIGURE 7: Langevin dipoles in the vicinity of Cluster I of *Pa*Fd. Shown are cluster (Fe, S*, and S_γ) atoms (dark spheres), the Langevin dipoles which occur within 6 Å of the cluster centroid (light spheres), and the ribbon trace of the polypeptide. The three Langevin dipoles above and to the left of the cluster fill a crevice bordered by C_γ and C_δ of Pro 47, C_β of Ala 13, S_γ of Cys 11, $C_{\delta 1}$ of Ile 9, and $C_{\gamma 2}$ of Val 46. The lone dipole below and to the right of the cluster fills a cavity defined by S_γ of Cys 14, the carbonyl of Gly 12, C_β of Lys 15, and $C_{\delta 2}$ of Tyr 29. This latter dipole lies just below the position of the observed water (WAT113 in coordinate set NEW).

significant changes in local backbone folding are induced by sequence changes will exhibit significant variations in redox potential from the parent proteins. The study of such mutants will be of great interest.

In addition to determining the folding of a protein around its $[Fe_4S_4^*Cys_4]$ cluster and, hence, the contribution of main-chain amide groups to its potential, the amino acid side chains of the protein affect the cluster potential more directly. Side-chain polarity contributes to $\Delta\upsilon_{Q\mu}$ and affects $\Delta\upsilon_{Q\alpha}$ and $\Delta\upsilon_L$ indirectly. Side-chain polarizability contributes to $\Delta\upsilon_{Q\alpha}$ and affects $\Delta\upsilon_L$ indirectly. Finally, side-chain size determines the availability of cavities of sufficient volume to permit the presence of Langevin dipoles, thus contributing to $\Delta\upsilon_L$. In comparing *Pa*Fd and *Av*FdI, proteins which, despite a substantial difference in sequence, exhibit very similar backbone folding around their $[Fe_4S_4^*Cys_4]$ clusters, our calculations have led to the conclusion that a major contribution to the difference in potential of Cluster I of *Pa*Fd and *Av*FdI arises from the presence of "local" Langevin dipoles in *Pa*Fd. Thus, in this specific case, the direct effect of the sequence differences between *Pa*Fd and *Av*FdI on $\Delta\upsilon_L$ predominates, and the effects on $\Delta\upsilon_{Q\mu}$ and $\Delta\upsilon_{Q\alpha}$ are less important.

While the presence of "local" water molecules in *Pa*Fd has not (so far) been experimentally verified, our calculations emphasize the potential importance of such water molecules in tuning the redox potentials of $[Fe_4S_4^*Cys_4]$ clusters, and of the role of side-chain groups in determining the availability of cavities suitable for their insertion. It is very likely that "local" water molecules will be found to contribute significantly

to the redox potentials of $[Fe_4S_4^*Cys_4]$ clusters in a substantial number of proteins. In particular, it is very likely that changes in $\Delta\upsilon_L$ due to changes in the "local" water population will be a major contributor to changes in redox potential induced by mutations. Studies of the redox potentials of mutants of *Pa*Fd and *Av*FdI in which "local" cavities, suitable for insertion of water molecules, have been created or destroyed will be of great interest.

Our PDLD calculations have not explicitly incorporated the charges of ionized or protonated residues or of charged prosthetic groups other than the one whose redox potential is under investigation. *Pa*Fd, *Av*FdI, and *Cv*HiPIP all contain a relatively large number of residues expected to be charged at the pH values near 7 at which redox potentials are measured. Both *Pa*Fd and *Av*FdI contain two [Fe-S] clusters in close proximity. Both cluster–cluster and cluster–charged residue interactions yield additional contributions to $\Delta\upsilon$ and to cluster redox potentials. Estimates of these contributions have been obtained macroscopically and lead to the conclusion that they are not of major significance. The values obtained are of course dependent on the value of the dielectric constant employed. The issue of the dielectric constant inside proteins has been (Rees, 1980; Warshel & Russell, 1984) and continues to be much debated. It is therefore important that direct experimental evidence can be adduced to support the conclusions arrived at theoretically. In the case of *Av*FdI, a number of mutants have recently been studied in which acidic residues have been replaced by neutral residues, or vice versa (Shen et al., 1993, 1994). This set includes D15N, D23N, H35D, E38S, E46A, and H35D/D41H. The redox potentials of the $[Fe_4S_4^*Cys_4]$ and $[Fe_3S_4^*Cys_3]$ clusters were unchanged (within experimental error), except in the cases of D15N where the potential of the $[Fe_3S_4^*Cys_3]$ cluster increased by ~20 mV and H35D/D41H where the potential of the $[Fe_4S_4^*Cys_4]$ cluster increased by ~20 mV. Residue 15 is very close to the $[Fe_3S_4^*Cys_3]$ cluster (Cys 16 is a ligand); residue 41 is similarly very close to the $[Fe_4S_4^*Cys_4]$ cluster (Cys 42 is a ligand). Also, it has been possible to prepare a chemically-modified form of *Av*FdI containing only the $[Fe_3S_4^*Cys_3]$ cluster: (3Fe)FdI (Stephens et al., 1985). The redox potential of the $[Fe_3S_4^*Cys_3]$ cluster is unchanged on removal of the $[Fe_4S_4^*Cys_4]$ cluster (unpublished results from these laboratories). Thus, there is now substantial experimental evidence that the charges of ionized and protonated residues and of other prosthetic groups do not contribute significantly to the redox potentials of [Fe-S] clusters.

The factors controlling the redox potentials of [Fe-S] proteins have been debated extensively [see, for example, Sweeney and Rabinowitz (1980) and Rees and Farrelly (1990)]. Attention has been particularly focused on cluster–protein hydrogen (H)-bonding and cluster "solvent accessibility". Comparison of the X-ray structures of *Pa*Fd and *Cv*HiPIP found substantially greater H-bonding by amide NH groups to cluster S^* and S_γ atoms in *Pa*Fd than in *Cv*HiPIP (Carter et al., 1974b; Adman et al., 1975), leading to the proposal that the large difference in the redox potentials of these two proteins, whose $[Fe_4S_4^*Cys_4]$ clusters are structurally indistinguishable (Carter et al., 1972), could be attributed to the difference in H-bonding. Subsequent discussions of [Fe-S] cluster redox potentials have continued to emphasize the contributions of H-bonding. For example, the difference in the potentials of the 2–/3– couple of the $[Fe_3S_4^*Cys_3]$ clusters of *Desulfovibrio gigas* ferredoxin II (*Dg*FdII) and *Av*FdI has recently been attributed to differential H-bonding to these clusters (Kissinger et al., 1991). In cases where differences in H-bonding do not appear to be the cause of differences in potentials, differential solvent accessibility has been invoked. For example, Backes et al. (1991) recently concluded that, in view of the strong structural homology between the environments of the $[Fe_4S_4^*Cys_4]$ clusters of *Pa*Fd, *Av*FdI, and *Bt*Fd—and of the H-bonding to these clusters in particular—the variation in potential of these clusters was most likely attributable to varying "solvent accessibility".

Our calculations support the conclusion that amide groups close to a cluster are of dominant importance in determining the cluster redox potential. However, the set of amide groups identifiable as H-bonding constitutes only a fraction of those of importance. In addition, the mechanism by which amide groups influence the redox potential is independent of whether or not the amide is engaged in H-bonding. The amide groups of *Pa*Fd and *Cv*HiPIP identified as H-bonding by Backes et al. (1991) belong to the sets listed in Table 6. In the case of Clusters I and II of *Pa*Fd these amides comprise 8 of the 15 listed in Table 6. In the case of *Cv*HiPIP they are 5 of the 7 listed in Table 6. Thus, the selection of the amide groups of importance on the basis of criteria pertaining to their H-bonding excessively constrains the identification of those amide groups of importance. Most dramatically, such a protocol completely ignores the contribution of amide groups close to the cluster, but oriented *un*favorably for H-bonding: in the case of Cluster I, amides 6 and 43; in the case of Cluster II, amides 15 and 33.

More fundamentally, our calculations show that, in modeling the contributions of amide groups to cluster redox potentials, explicit inclusion of H-bonding is unnecessary. Our model assumes that the cluster–amide interaction is the sum of charge–charge and charge-induced dipole contributions; specific H-bonding terms are excluded from the cluster–protein interaction potential. The success of our calculations supports the view that these assumptions are reasonable and that the exclusion of explicit consideration of H-bonding is not a substantial deficiency.

It could be argued that, even if not defined as such, the Coulombic interaction of a cluster S atom and an amide NH group constitutes *de facto* a H-bond. Even if such a semantic proposition were to be accepted, and the contributions of all S···HN interactions by amides exhibiting S···N distances <4 Å were to be defined as H-bonding contributions, H-bonding would still be of limited importance. First, the Coulombic interactions of a given amide NH group with the entire cluster are much greater than that of the one (or at most two) cluster S atoms engaged in H-bonding. Second, the contribution of the CO moiety of the amide group is comparable to that of the NH moiety.

There are of course other difficulties associated with the interpretation of redox potentials in terms of cluster H-bonding. First, the criteria by which H-bonding is identified are not uniquely defined, and different papers use different criteria. Second, attempts to provide a simple, linear quantitative relationship between potential and H-bonding [such as that proposed by Carter (1977b)] ignore the wide variation in H-bonding among amide groups consequent on the wide variation in N···S distances, N—H···S deviations from collinearity, and H-bonding structures (simple, bifurcated, etc.).

While "solvent accessibility" has been frequently cited as a contributing factor to [Fe-S] cluster redox potentials, the difficulty both of defining and measuring "solvent accessibility" and of evaluating its effect on redox potentials has precluded

firm conclusions as to its importance. Indirect evidence regarding "solvent accessibility" has been provided by studies of the kinetics of D and T exchange of H atoms in the vicinity of [Fe-S] clusters (Adman et al., 1975). Direct evidence is in principle provided by X-ray crystallography. However, even the most recent and detailed comparison of the X-ray structures of *Pa*Fd and *Av*FdI has not succeeded in demonstrating differential "solvent accessibility" of their $[Fe_4S_4^*Cys_4]$ clusters (Merritt et al., 1993).

Our calculations provide a specific, theoretical solvent model which, *inter alia*, provides a well-defined measure of "solvent accessibility". In addition, the contribution of the solvent to the redox potential of a cluster is calculated quantitatively. The prior suggestions that differences in "solvent accessibility" can contribute significantly to differences in redox potential are supported by our work. At the same time, the limitations of a solvent model consisting of a point dipole grid, together with the paucity of experimental data regarding solvent molecules near clusters, clearly mandate continued study of this topic both theoretically and experimentally. In particular, extension of the calculational methodology to include the atoms of (at least some) water molecules at the same level as protein atoms is clearly extremely important. From the experimental standpoint, increased resolution of X-ray structures to locate ordered solvent molecules more definitively and in greater number and increased application of magnetic resonance techniques [ENDOR, ESE (Orme-Johnson et al., 1983; Malikayil et al., 1985), NMR, etc.] are clearly important.

CONCLUSION

The calculation of the tuning of the redox potential of a prosthetic group by its protein environment requires a model of sufficient sophistication, incorporating all essential physics, whose implementation is practicable. The PDLD model used here treats both the protein and the aqueous solvent microscopically. It incorporates not only the charges of protein atoms, but also their polarizabilities. It not only treats solvent water microscopically but also treats interstitial and bulk water in a uniform manner. The essential physics of the electrostatic interaction of the prosthetic group and its environment is thus included. At the same time, the modeling of water molecules as a grid of Langevin dipoles makes calculations using large numbers of water molecules practicable. The treatment of solvent water as a macroscopic continuum dielectric, although simpler than the microscopic approach of the PDLD model, cannot treat interstitial water which, as we have illustrated in this work, can be of substantial importance. The treatment of solvent water at the atomic level is at present extremely demanding calculationally. For the time being, the PDLD model is therefore an optimum choice.

The results presented in this paper support the utility of the PDLD model. The ordering and spacing of the redox potentials of the 2–/3– couples of the $[Fe_4S_4^*Cys_4]$ clusters of *Pa*Fd, *Av*FdI, and *Cv*HiPIP are qualitatively reproduced, with the exception of Cluster II of *Pa*Fd. Analysis of the calculations illuminates the mechanisms by which the redox potentials of $[Fe_4S_4^*Cys_4]^{2-/3-}$ clusters—and, by extension, all [Fe-S] clusters—are tuned by their protein environment. Most importantly, new light is shed on the contributions of main-chain amide groups and of water molecules close to a cluster.

While these initial results are very encouraging, the PDLD methodology clearly requires both further evaluation and further development. Calculations on other proteins expressing the $[Fe_4S_4^*Cys_4]^{2-/3-}$ couple and on proteins expressing other [Fe-S] clusters and couples will be reported in the near future. At the same time, a more thorough study of the importance of Molecular Dynamics averaging of PDLD calculations is under way. In the future, we also plan to extend the solvent model to treat some fraction of solvent molecules at the atomic level.

ACKNOWLEDGMENT

We are grateful to R. Langen, Z. T. Chu, L. Manna, F. J. Devlin, D. R. Jollie, and C. D. Stout for discussions and technical assistance; to Professor E. T. Adman for communicating the NEW coordinates of *Pa*Fd prior to publication; and to Dr. L. Noodleman for communicating the results of DF calculations prior to publication. This work was supported in part by NIH Grants # GM 45209 and 40283.

REFERENCES

Adams, M. W. W. (1992) in *Iron–Sulfur Proteins* (Cammack, R., Ed.) *Advances in Inorganic Chemistry*, Vol. 38, pp 341–396, Academic Press.

Adman, E. T., Siecker, L. C., & Jensen, L. H. (1973) *J. Biol. Chem. 248*, 3987–3996.

Adman, E. T., Watenpaugh, K. D., & Jensen, L. H. (1975) *Proc. Natl. Acad. Sci. U.S.A. 72*, 4854–4858.

Adman, E. T., Sieker, L. C., & Jensen, L. H. (1976) *J. Biol. Chem. 251*, 3801–3806.

Backes, G., Mino, Y., Loehr, T. M., Meyer, T. E., Cusanovich, M. A., Sweeney, W. V., Adman, E. T., & Sanders-Loehr, J. (1991) *J. Am. Chem. Soc. 113*, 2055–2064.

Bartsch, R. G. (1963) in *Bacterial Photosynthesis* (San Pietro, A., Gest, H., & Vernon, L. P., Eds.) p 315, Antioch Press, Yellow Springs, OH.

Cammack, R. (1973) *Biochem. Biophys. Res. Comm. 54*, 548–554.

Cammack, R., Ed. (1992a) *Iron–Sulfur Proteins, Advances in Inorganic Chemistry*, Vol. 38, Academic Press.

Cammack, R. (1992b) in *Iron–Sulfur Proteins* (Cammack, R., Ed.) *Advances in Inorganic Chemistry*, Vol. 38, pp 281–322, Academic Press.

Carter, C. W. (1977a) in *Iron-Sulfur Proteins* (Lovenberg, W., Ed.) Vol. III, Chapter 6, pp 157–204, Academic Press.

Carter, C. W. (1977b) *J. Biol. Chem. 252*, 7802–7811.

Carter, C. W., Kraut, J., Freer, S. T., Alden, R. A., Sieker, L. C., Adman, E., & Jensen, L. H. (1972) *Proc. Natl. Acad. Sci. U.S.A. 69*, 3526–3529.

Carter, C. W., Kraut, J., Freer, S. T., Xuong, N. H., Alden, R. A., & Bartsch, R. G. (1974a) *J. Biol. Chem. 249*, 4212–4225.

Carter, C. W., Kraut, J., Freer, S. T., & Alden, R. A. (1974b) *J. Biol. Chem. 249*, 6339–6346.

Chen, J. L., Mouesca, J. M., Noodleman, L., Case, D. A., & Bashford, D. (1993) *J. Inorg. Biochem. 51*, 449.

Churg, A. K., & Warshel, A. (1986) *Biochemistry 25*, 1675–1681.

Cutler, R. L., Davies, A. M., Creighton, S., Warshel, A., Moore, G. R., Smith, M., & Mauk, A. G. (1989) *Biochemistry 28*, 3188–3197.

Freer, S. T., Alden, R. A., Carter, C. W., & Kraut, J. (1975) *J. Biol. Chem. 250*, 46–54.

Fukuyama, K., Nagahara, Y., Tsukihara, T., & Katsube, Y. (1988) *J. Mol. Biol. 199*, 183–193.

Fukuyama, K., Matsubara, H., Tsukihara, T., & Katsube, Y. (1989) *J. Mol. Biol. 210*, 383–398.

George, S. J., Armstrong, F. A., Hatchikian, E. C., & Thomson, A. J. (1989) *Biochem. J. 264*, 275–284.

Georgiadis, M. M., Komiya, M., Chakrabarti, P., Woo, D., Kornuc, J. J., & Rees, D. C. (1992) *Science 257*, 1653–1659.

Hase, T., Ohmiya, N., Matsubara, H., Mullinger R. N., Rao, K. K., & Hall, D. O. (1976) *Biochem. J. 159*, 55–63.

Howard, J. B., & Rees, D. C. (1991) *Adv. Protein Chem. 42*, 199–280.

Iismaa, S. E., Vazquez, A. E., Jensen, G. M., Stephens, P. J., Butt, J. N., Armstrong, F. A., & Burgess, B. K. (1991) *J. Biol. Chem. 266*, 21563–21571.

Kennedy, M. C., & Stout, C. D. (1992) in *Iron-Sulfur Proteins* (Cammack, R., Ed.) *Advances in Inorganic Chemistry*, Vol. 38, pp 323–339, Academic Press.

Kissinger, C. R., Sieker, L. C., Adman E. T., & Jensen, L. H. (1991) *J. Mol. Biol. 219*, 693–715.

Krishnamurthy, H. M., Hendrickson, W. A., Orme-Johnson, W. H., Merritt, E. A., & Phizackerley, R. P. (1988) *J. Biol. Chem. 263*, 18430–18436.

Langen, R., Brayer, G. D., Berghuis, A. M., McLendon, G., Sherman, F., & Warshel, A. (1992a) *J. Mol. Biol.* 224, 589–600.

Langen, R., Jensen, G. M., Jacob, U., Stephens, P. J., & Warshel, A. (1992b) *J. Biol. Chem. 267*, 25625–25627.

Lee, F. S., Chu, Z. T., & Warshel, A. (1993) *J. Comput. Chem. 14*, 161–185.

Lim, L. W., Shamala, N., Mathews, F. S., Steenkamp, D. J., Hamlin, R., & Xuong, N. H. (1986) *J. Biol. Chem. 261*, 15140–15146.

Lovenberg, W., Ed. (1973a) *Iron-Sulfur Proteins* Vol. I, Academic Press.

Lovenberg, W., Ed. (1973b) *Iron-Sulfur Proteins* Vol. II, Academic Press.

Lovenberg, W., Ed. (1977) *Iron-Sulfur Proteins* Vol. III, Academic Press.

Malikayil, J. A., Sweeney, W. V., McCracken, J., & Peisach, J. (1985) *Biochem. Biophys. Res. Commun. 133*, 1119–1124.

Matsubara, H. & Saeki, K., (1992) in *Iron–Sulfur Proteins* (Cammack, R., Ed.) *Advances in Inorganic Chemistry*, Vol. 38, pp 223–280, Academic Press.

Merritt, E. A., Stout, G. H., Turley, S., Sieker, L. C., Jensen, L. H., & Orme-Johnson, W. H. (1993) *Acta Crystallogr. D49*, 272–281.

Mizrahi, I. A., Wood, F. E., & Cusanovich, M. A. (1976) *Biochemistry 15*, 343–348.

Mouesca, J. M., Chen, J. L., Noodleman, L., Bashford, D., & Case, D. A. (1994) (submitted for publication).

Mulliger, R. N., Cammack, R., Rao, K. K., Hall, D. O., Dickson, D. P. E., Johnson, C. E., Rush, J. D., & Simopoulos, A. (1975) *Biochem. J. 151*, 75–83.

Noodleman, L., Norman, J. G., Osborne, J. H., Aizman, A., & Case, D. A. (1985) *J. Am. Chem. Soc. 107*, 3418–3426.

Orme-Johnson, N. R., Mims, W. B., Orme-Johnson, W. H., Bartsch, R. G., Cusanovich, M. A., & Peisach, J. (1983) *Biochim. Biophys. Acta 748*, 68–72.

Pace, C. P. & Stankovich, M. T. (1991) *Arch. Biochem. Biophys. 287*, 97–104.

Parson, W. W., Chu, Z. T., & Warshel, A. (1990) *Biochim. Biophys. Acta 1017*, 251–272.

Rall, S. C., Bolinger, R. E., & Cole, R. D. (1969) *Biochemistry 8*, 2486–2496.

Rees, D. C. (1980) *J. Mol. Biol. 141*, 323–326.

Rees, D. C. & Farrelly, D. (1990) in *The Enzymes* (Sigman, D. S. & Boyer, P. D., Eds.) Vol. 19, Chapter 2, pp 37–97, Academic Press.

Russell, S. & Warshel, A. (1985) *J. Mol. Biol. 185*, 389–404.

Shen, B., Martin, L. L., Butt, J. N., Armstrong, F. A., Stout, C. D., Jensen, G. M., Stephens, P. J., LaMar, G. N., Gorst, C. M., & Burgess, B. K. (1993) *J. Biol. Chem. 268*, 25928–25939.

Shen, B., Jollie, D. R., Stout, C. D., Diller, T. C., Armstrong, F. A., Gorst, C. M., La Mar, G. N., Stephens, P. J., & Burgess, B. K. (1994) *J. Biol. Chem. 269*, 8564–8575.

Spiro, T. G. (1982) *Iron-Sulfur Proteins*, Vol. IV, Academic Press.

Stephens, P. J., Morgan, T. V., Devlin, F. J., Penner-Hahn, J. E., Hodgson, K. O., Scott, R. A., Stout, C. D., & Burgess, B. K. (1985) *Proc. Natl. Acad. Sci. U.S.A. 82*, 5661–5665.

Stephens, P. J., Jensen, G. M., Devlin, F. J., Morgan, T. V., Stout, C. D., Martin, A. E., & Burgess, B. K. (1991) *Biochemistry 30*, 3200–3209.

Stombaugh, N. A., Sundquist, J. E., Burris, R. H., & Orme-Johnson, W. H. (1976) *Biochemistry 15*, 2633–2642.

Stout, C. D. (1988) *J. Biol. Chem. 263*, 9256–9260.

Stout, C. D. (1989) *J. Mol. Biol. 205*, 545–555.

Stout, C. D. (1993) *J. Biol. Chem. 268*, 25920–25927.

Stout, G. H., Turley, S., Sieker, L. C., & Jensen, L. H. (1988) *Proc. Natl. Acad. Sci. U.S.A. 85*, 1020–1022.

Sweeney, W. V., & Magliozzo, R. S. (1980) *Biopolymers 19*, 2133–2141.

Sweeney, W. V., & Rabinowitz, J. C., (1980) *Annu. Rev. Biochem. 49*, 139–161.

Tranqui, D., Fanchon, E., Vicat, J., Sieker, L. C., Meyer J., Moulis, J. M., Gagnon, J., & Duee, E. (1991) *International Conference on Bioinorganic Chemistry (ICBIC) V*, Abstract D049, Oxford, U.K.

Warshel, A., & Russell, S. T. (1984) *Q. Rev. Biophys. 17*, 283–422.

Warshel, A., & Creighton, S. (1989) in *Computer Simulation of Biomolecular Systems* (Van Gunsteren, W. F., and Weiner, P. K., Eds.) pp 120–138, ESCOM, Leiden, The Netherlands.

Watt, G. D., Wang, Z. C., & Knotts, R. R. (1986) *Biochemistry 25*, 8156–8162.

Yoch, D. C., & Arnon, D. I. (1972) *J. Biol. Chem. 247*, 4514–4520.